Ductile Fracture Criterion Comparisons & Development of a Numerical Material Damage Model

Mark Krueger

University of Minnesota

Abstract*: By using Abaqus finite element software, contributions to understanding and quantifying the ductile fracture behavior of metallic materials have been realized. The end result has enhanced product development by reducing unnecessary conservatism resulting in reduced failure rates, product weight, and costs. Unlike the methods of LEFM or EPFM which presume a pre-existing flaw, the ductile fracture approach requires no initial flaw size, shape, or flaw orientation relative to the component geometry. In this paper, numerical examples using various damage approaches are used to highlight differences in their resulting failure modes. In addition, the use of a damage model on a practical example is used to emphasize the utility of the method.*

Keywords*: damage, ductile, failure, fracture, impact, response surface method, rupture.*

1. Introduction

1.1 Overview

Numerical simulations of the mechanical response for ductile materials are common among the engineering industry. It is also common to use traditional metrics in the assessment of material failure (i.e. rupture). While these traditional methods are often conservative and seemingly less costly (at least initially), they are unable to provide the actual magnitude of conservatism in the results because of the assumptions that are typically employed. This results in components being over-designed in order to meet safety and functional requirements.

The use of 'damage' as a metric within numerical simulations is a viable alternative to better represent the materials behavior at failure. While this approach is phenomenological, this paper will demonstrate its utility and outline the process used to develop a damage model suitable for use in Abaqus.

The method employed herein uses traditional continuum elements without the need to introduce XFEM into the analysis process which is applicable for assessing a given geometric discontinuity. The damage metric is part of the material property definition and can use existing damage models built into Abaqus such as a tabular function. Another option is to incorporate a user defined model via FORTRAN subroutines of which some of the examples in this paper have used. This is accomplished using a field variable dependent material property subroutine VUSDFLD to define the material damage response.

It should be noted that when discussing the topic of material damage, there can be a difference between the academic and industrial perspectives. In industry, we are typically employing a phenomenological approach which is macroscopic viewpoint. In much of the academic research, 1st principles of physics are frequently employed for predictive purposes and can replicate the dislocations at the atomic level. In order to do this, atomistic simulations of individual atoms are modeled of which one of these methods is the quasi-continuum method (Tadmor et.al, 2011). This particular method uses a mesh that transitions from individual atoms to a more traditional finite element mesh.

1.2 Scope

Within this paper there are a number of assumptions that are presumed. However, these limitations are not so restrictive as to make the method a 'research project' as it has been successfully implemented by the author on industry products. Summarizing these assumptions:

- Loading – the loading is monotonic resulting in deformation well beyond 'moderate' yielding. Therefore, we are not concerned about cyclical loads such as those exhibited for fatigue analysis. Also, there are no residual stresses or strains that would affect the damage process.
- Material behavior – the materials considered are ductile metallic alloys which are homogenous and isotropic with properties representative of bulk materials with a polycrystalline structure without any pre-existing flaws. In addition, the material constitutive model used is load-rate independent in its response. For many materials, this type of approximation is often adequate even when the loading is ballistic with the material response only varying 5%.
- Failure mode – the failure is that of ultimate failure where the material ruptures (i.e. fractures). The failure considered here is not limited by load carrying capacity, instability, buckling, or other modes that may be applicable to the design process of a product.

1.3 Isotropic Plasticity

Given the aforementioned scope, the Von Mises yield model is used. This yield criterion is independent of the hydrostatic pressure and is both a symmetric and even function using a hardening rule expanding the yield surface equally in all directions as plastic flow occurs. Figure 1 illustrates an isometric view of three-dimensional principle stress space for this material yield model.

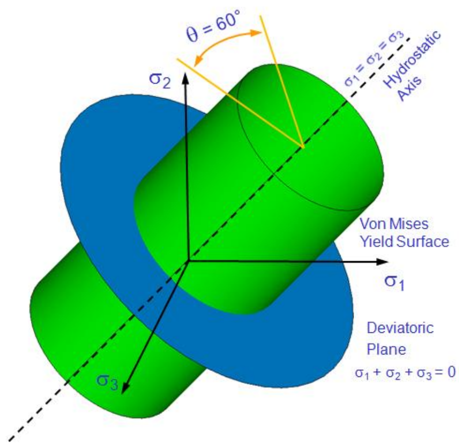

Figure 1. Isotropic Material Yield Surface.

For this material yield model, the following quantities are used to define the location on the yield/failure cylinder surface for a given stress tensor:

The hydrostatic stress:

$$p = \frac{-1}{3}(\sigma_1 + \sigma_2 + \sigma_3) = \frac{-1}{3} tr[\boldsymbol{\sigma}] \tag{1}$$

The equivalent stress determined from the deviatoric stress tensor:

$$q = \sqrt{\frac{3}{2} \cdot \boldsymbol{s}:\boldsymbol{s}} \tag{2}$$

The triaxiality:

$$\eta = \frac{-p}{q} \tag{3}$$

The 3rd deviatoric invariant:

$$r = \left(\frac{9}{2} \cdot \boldsymbol{s} \cdot \boldsymbol{s}:\boldsymbol{s}\right)^{\frac{1}{3}} = \left(\frac{27}{2} det(\boldsymbol{s})\right)^{\frac{1}{3}} \tag{4}$$

The normalized Lode angle, ranging between -1 and +1:

$$\xi = \left(\frac{r}{q}\right)^3 = cos(3\theta) \tag{5}$$

1.4 Common Measures of Material Failure

To give an indication of validity of a design, a margin of safety is typically calculated using a metric of a representative ‘applied’ response which is then compared to an ‘allowable’ value. After selecting a metric, there are two general issues of concern:

1. Applied value – from the FEA results, what tensor component, invariant, or principal value should be used that describes the condition of the material response in a comprehensive fashion? For a complex load state, this may not be so obvious.
2. Allowable value – since the applied value needs to be compared to some reference value, does the allowable value represent the same material load conditions?

One of the most common measures used to assess material failure is *stress*, which for large deformations would be the Cauchy stress. This is then compared to an allowable strength which is frequently the material ultimate tensile strength (UTS). Based on engineering experience, for decades engineering design manuals have successfully employed this criterion to determine ductile material failure from the normality and associative requirements for an isotropic material model under multi-axial loading. With the stress being the dependent variable, scaling the margin of safety to material fracture can be misleading because of the non-linearity and it can also ignore a significant portion of the material capacity to absorb energy illustrating a limitation.

A second significant limitation of using a stress measure is that of resolution. Since stresses are derived from the strain using a constitutive material model, a small change in strain ($\Delta\varepsilon_{y-}$) can give reasonable stress output resolution ($\Delta\sigma_{y-}$) when we are in the elastic region as illustrated in Figure 2 below. However, if the response is in the nonlinear region beyond the yield point, for even a large change in the strain ($\Delta\varepsilon_{y+}$) we may only observe a very small change in the stress response ($\Delta\sigma_{y+}$) making it harder to be accurate if using a stress measure to determine material failure.

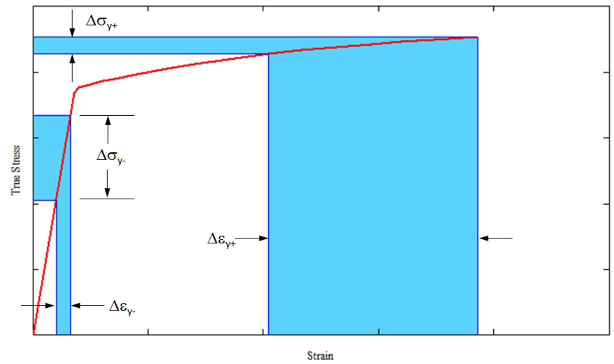

Figure 2. Stress-strain Resolution.

Another measure that is often used to assess material failure is *strain*. One advantage of using strain rather than stress when calculating a margin, is that you're using the independent variable. So for any scaling of the result it is linear giving a more intuitive representation of the margin.

2. Damage

For many engineering applications, classical plasticity theory works just fine. However, if the response is beyond moderate plasticity as considered here, the changes in the microstructure are no longer insignificant but play an important role in predicting material failure.

Using parameters such as the triaxiality, the strain rate, temperature, and Lode angle, contemporary damage models generally fall into two general categories:

1. The first is a *conventional continuum mechanics* model where the damage process is independent of the material behavior and the plastic properties are unaltered. The Johnson-Cook model is an example of this.
2. The second category is a *continuum damage mechanics* model where the damage process is dependent on material behavior and is coupled to the plasticity. This type of model is where most research is being done.

2.1 Damage Model Analytical Comparisons

The following seven failure criteria in Table 1 are used to make comparisons and highlight some of the differences between them. One of these compared includes a user-defined model which incorporates both the triaxiality and Lode angle parameters.

Table 1. Compared Methods of Failure Criteria.

I.	User-defined	V.	Johnson-Cook
II.	Maximum shear stress	VI.	Equivalent strain
III.	Cockroft-Latham	VII.	FLD
IV.	Wilkins		

In Figure 3 below, the selected criterion are compared by looking at principal stress space under plane-stress conditions. Normalized principal stresses are used for each of the axes. Note that the difference between the criteria is practically negligible under shear loading. Some of the greatest differences occur under plane strain condition but most follow a similar curvature in this region with little difference between them resulting in little significance for practical considerations.

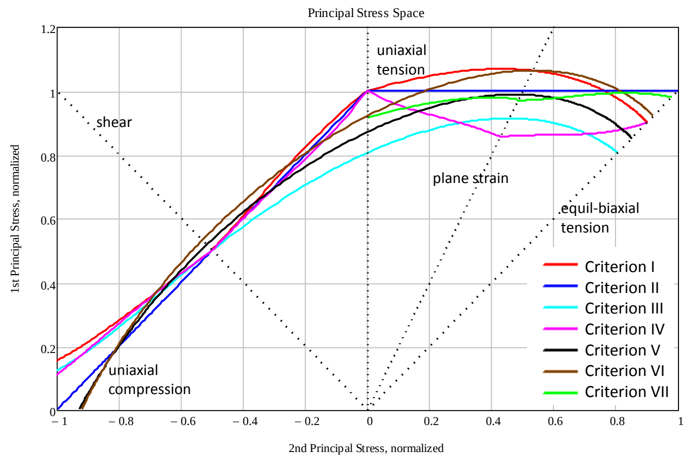

Figure 3. Damage Model Comparison in Principal Stress Space.

Again making a similar contrast, in Figure 4 the same failure criteria are now plotted in principal strain space for plane-stress conditions. Normalized principal strains are used for each of the axes. Some of the differences between the failure criteria become more prominent. This illustrates a 'resolution' problem using stress as a failure measure. This also supports the use of strain as failure measure rather than using stress by providing greater fidelity in the assessment.

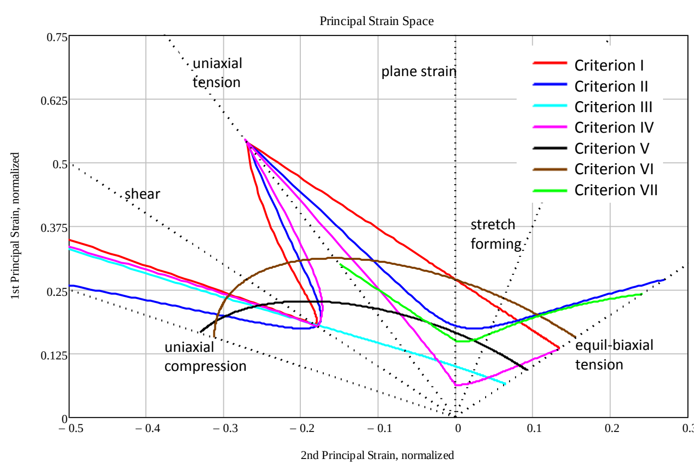

Figure 4. Damage Model Comparison in Principal Strain Space.

In Figure 5 the same seven damage criteria are again contrasted for plane-stress conditions plotted in equivalent strain-triaxiality space with the failure strain being a function of the triaxiality. This again further highlights difference in the criteria and illustrating a failure strain metric being preferable as contrasted to using principal stress-space.

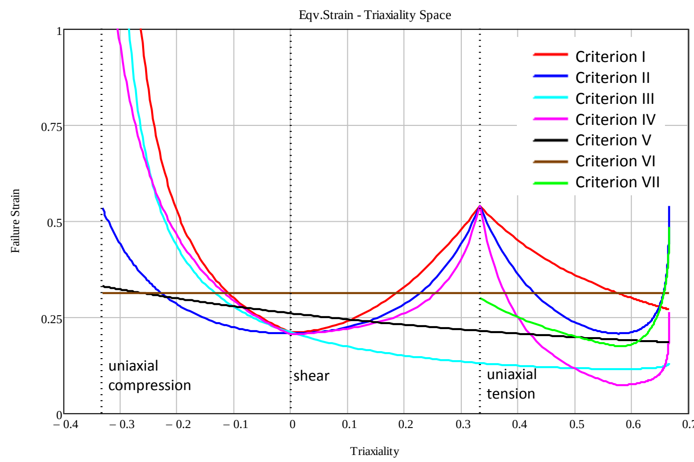

Figure 5. Damage Model Comparison in Equivalent Strain-triaxiality Space.

2.2 Abaqus Implementation of Damage

In addition to incorporating a variety of plasticity models, Abaqus provides a variety of numerical methods to define ‘failure’ which includes concrete and composite materials, connector elements, as well as that for bulk materials. The scope herein uses the isotropic material model and a progressive damage model for ductile materials.

Similar to what can be found in the Abaqus documentation (Abaqus User’s Manual) regarding damage definition, the plot in Figure 6 illustrates some of the damage parameter relationships relative to the stress-strain curve.

- The region from 'a' to 'b' is the linear elastic region.
- The region from 'b' to 'c' illustrates plastic flow and strain hardening.
- The region from point 'c' to 'd' defines the damage evolution with point ‘c’ defining the damage initiation parameter.
- The region from point 'c' to 'd`' is an undegraded material response.

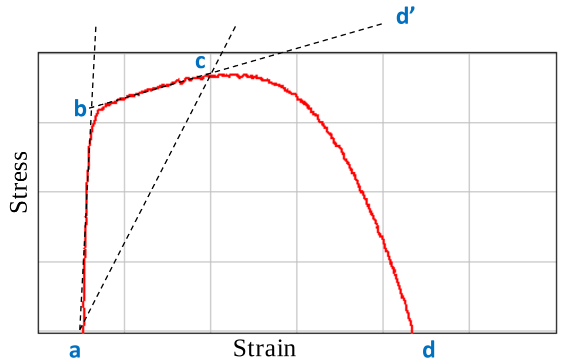

Figure 6. Damage Definition Effect on Stress-strain Response.

The fracture energy (G_f) used in the damage evolution definition is related to the plastic strain ($\bar{\varepsilon}^{pl}$) or alternatively the plastic displacement ($\bar{u}^{pl}$):

$$G_f = \int_{\bar{\varepsilon}_o^{pl}}^{\bar{\varepsilon}_f^{pl}} L\sigma_y d\bar{\varepsilon}^{pl} = \int_0^{\bar{u}_f^{pl}} \sigma_y d\bar{u}^{pl} \tag{6}$$

3. Numerical Case Studies

A series of numerical examples using Abaqus are used to demonstrate differences in damage model results using common test specimen geometries as well as an impact example.

This first example is a tensile specimen composed of an aluminum alloy. Three different damage models are compared: a constant failure strain model, the Johnson-Cook model, and a user-defined model. In Figure 7, contours of the damage initiation are contrasted. Note the similarity between the constant strain and Johnson-Cook models which fail in an almost brittle fashion. Only the user defined damage model correctly reflected both the test results force deflection curve and cup-and-cone failure mode.

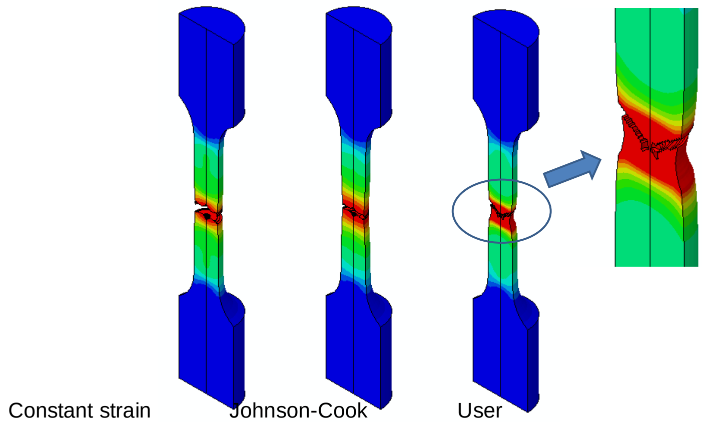

Figure 7. Damage Initiation Comparisons for Tensile Test Specimen.

A second example using a 3-point bend specimen composed of an aluminum alloy compares the Johnson-Cook model and a user-defined damage model. In Figure 8, contours of the damage degradation are contrasted. Note that the Johnson-Cook model didn't fail at all under the prescribed loading. The user defined damage model again correctly reflected both the test results force-deflection curve and the failure mode which included a shear lip.

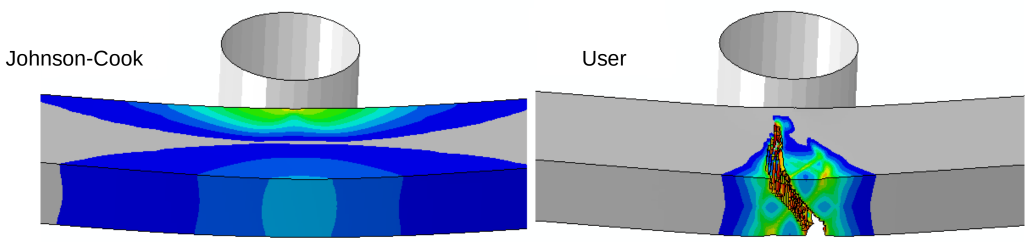

Figure 8. Damage Degradation Comparison for 3-Point Bend (bottom view).

A third example of an hourglass compression test specimen composed of an aluminum alloy compares the Johnson-Cook model and the user-defined damage models. In Figure 9, contours of the damage degradation are contrasted. Note that the Johnson-Cook model fails horizontally across the specimen neck in a brittle mode fracturing prematurely relative to the test data force-deflection curve. The user defined damage model correctly reflected both the test results force deflection curve and the failure mode by fracturing in a slanted orientation.

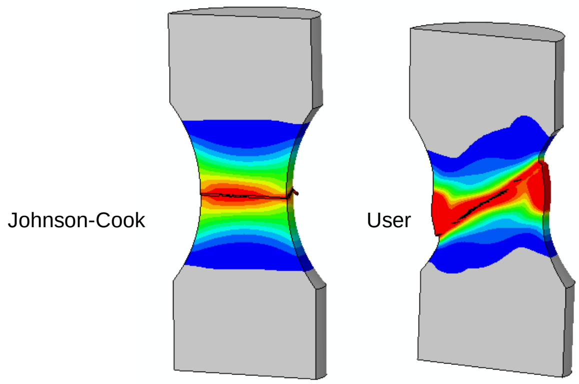

Figure 9. Damage Degradation Comparison of Compression Specimen (Cutview).

A fourth example of a rigid body impactor given an initial velocity contacting an aluminum beam contrasts the constant failure strain, Johnson-Cook, and user-defined damage models. In Figure 10, the beam deformation mode is contrasted. Note the similarity between the constant strain and Johnson-Cook models which disintegrates a large portion of the elements in the beam. The user-defined model correctly matches test results showing a shear plugging failure mode. Similar differences between the failure modes were observed using other impactor shapes composed of blunt or ogive geometries.

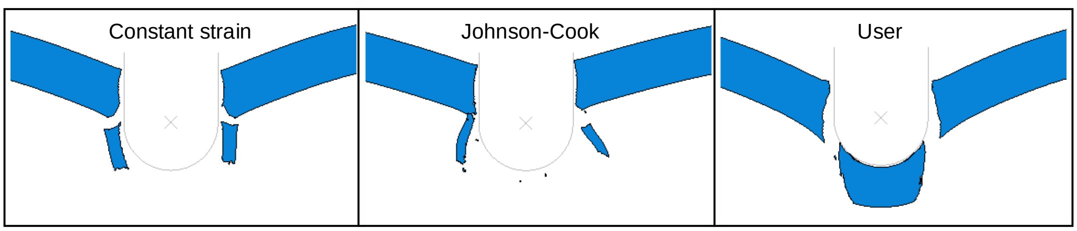

Figure 10. Damage Model Impact Failure Mode Comparison.

With the failed elements colored in blue in Figure 11, the effect on the failure mode by different impact velocities is assessed. This transition in the beam failure mode was correctly captured by the user model but was not for the constant failure strain or Johnson-Cook damage models.

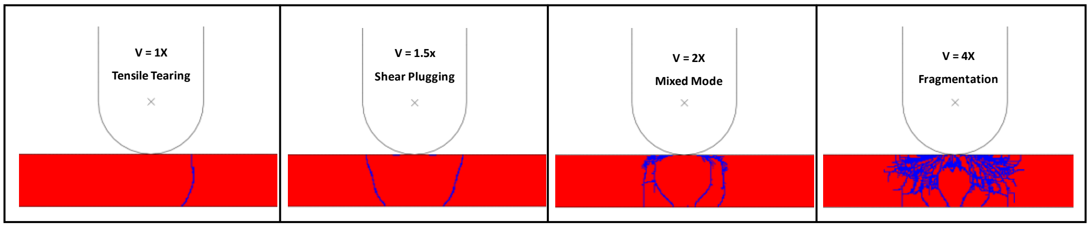

Figure 11. User Model Failure Mode Transition Comparison.

3.1 Summary

For numerical simulations, the use of stress is not preferred as a failure metric in part due to the dependence on the constitutive model and the resolution of the response. Similarly, using a constant strain damage model provides the analyst a simple method to 'fail' a material but has been demonstrated to be lacking in its ability to correctly match test results.

Beyond a constant strain model, the ground-breaking work by Johnson and Cook provided a more advanced damage model for numerical simulations. It is attractive in its use because of the current availability of material properties, direct incorporation into commercial software, and is familiar to many often making the numerical results more readily acceptable. One of the limitations noted in the literature for this model is that the specific material models may have been created using only two data points without encompassing the full range of triaxiality. Similarly, some of the material properties were calibrated from tensile tests alone giving unrealistic results for compressive dominated loading.

In contrast to the Johnson and Cook conventional continuum model, a user-defined continuum damage model has been shown to provide more accurate and comprehensive results over various test methods and geometries.

4. Damage Model Development

To develop the user-defined damage model similar to those used in the previous examples, a series of material tests and numerical simulations for correlation purposes is performed in two phases. The first phase correlates the stress-strain response & the second phase correlates damage response.

4.1 Stress-strain Characterization

To characterize the stress-strain curve, a variety of test specimen geometries are machined and tested. These are used to develop and correlate both the stress-strain curve and damage models.

The resulting stress-strain model should result in similar force-deflection curves for the various specimens as illustrated below in Figure 12.

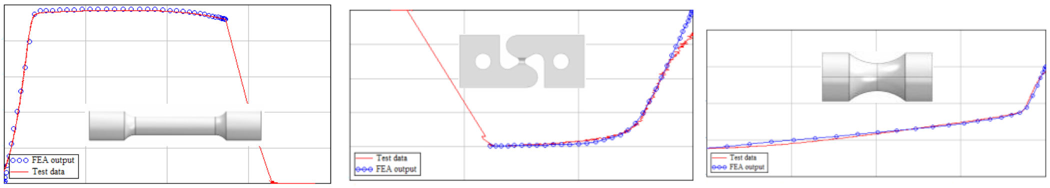

Figure 12. Sample Force-displacement Correlation.

4.2 Damage Characterization

To obtain the second material test correlation objective, the triaxiality and Lode angle space must be populated with data points of material fracture. The numbers of data points must be sufficient to be able to create a surface fit of the results and provide the desired fidelity of the failure model. Using the correlated stress-strain curve and by knowing the triaxiality and Lode angle for each type of specimen, the damage initiation and damage evolution values are adjusted to match the test data fracture strain to obtain a single unified damage model. Some of the results for the various types of specimens are illustrated below in Figure 13 with the red curve indicating plane-stress conditions.

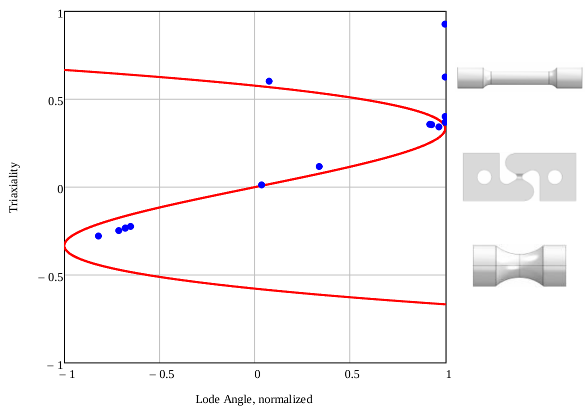

Figure 13. Population of the Two-parameter Data Space.

Once the numerical material model has been fully correlated, a surface fit is created which represents the material failure over a sector. Because currently there isn't a universal equation to describe the response surface, each material must be individually characterized. The functional form describing the surface response may vary by using appropriate functions that minimize the error but are still tractable based on the available data points and the desired fidelity. Using the developed surface fit, it is then reflected and subsequently repeated as a pattern around the hydrostatic axis. These steps are illustrated below in Figure 14 showing the initial surface fit to the data points and the final material fracture strain model plotted in principal strain space. Note the dependence of the surface as a function of the pressure along the hydrostatic axis and also the Lode angle tangentially around the hydrostatic axis. This failure surface illustrates a sharp contrast to the cylindrical or hexagonal failure surface using a Tresca or Mises model with the latter previously illustrated in Figure 1.

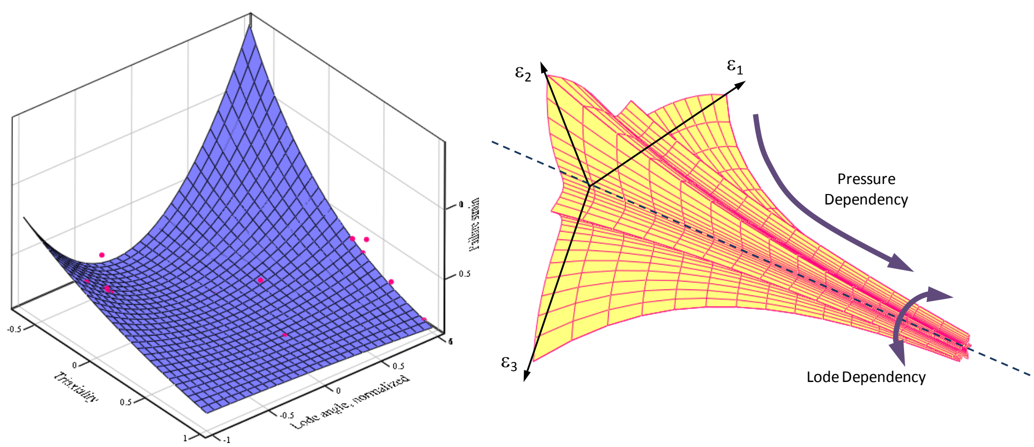

Figure 14. Surface Fit of Failure Data.

5. Application Example

To illustrate the use of the described damage approach, an example of drawing a circular flat plate with three successive ironing passes is used. In addition to the draw, each operation simulated includes the necessary tooling to simulate the manufacturing process. The plate blank is composed of a copper alloy material and uses an isotropic, power-law hardening model. The principal objective of the analysis is to determine the plastic strain response as a function of both the friction factor and the hardening exponent. This response is obtained by developing a surface plot over a range of conditions for each of the simulated manufacturing stations. Additional benefits of the analysis include verification of: hand calculations, final deformed shape, required number of required stations, reaction loads, etc.

In Figure 15 below, the sequence of simulated manufacturing stations is depicted starting with the initial cup draw. Subsequent to the draw, there are 3 series of ironing stations each one starting with the deformed geometry from the previous step. Example plastic strain results for specific parameters are also illustrated in Figure 15 for each station.

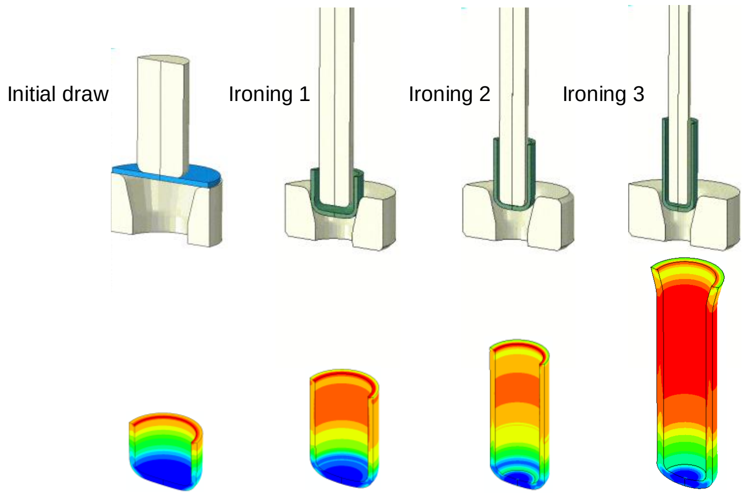

Figure 15. Drawing Steps Overview with Sample Plastic Strain Results.

For each manufacturing station, a response surface is created by populating the space with the peak plastic strain results in order to determine optimal conditions. Figure 16 below illustrates an example surface plot of the plastic strain response as a function of the independent variables for one of the manufacturing stations.

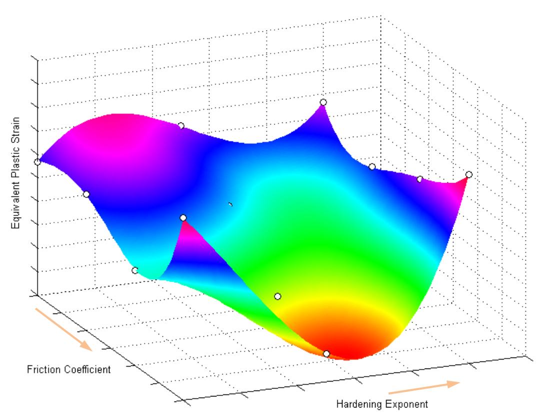

Figure 16. Drawing Station Plastic Strain Surface Response.

Using the Abaqus FEA results, a comparison of various damage criteria are illustrated below in Figure 17. The Forming Limit Diagram and Fracture Forming Limit Diagram are common assessment methods (Tang et.al, 2007) employed on similar problems such as this, as well as some of the aforementioned criterion. As it turns out, only the user routine, FFLD, and maximum shear models correctly predict that the material won't fail while the others do not.

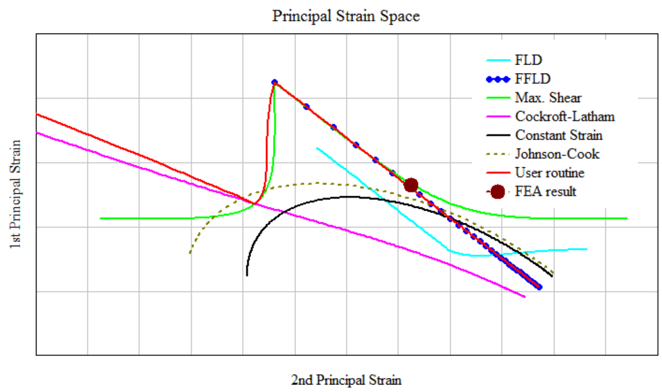

Figure 17. Failure Methodology Results Comparison.

6. Conclusion

The basic concept of using damage as a metric to describe material failure has been discussed with some comparisons made to the more traditional metrics of stress or strain. Various material damage models were also contrasted to illustrate some of the variations in response using common test specimen geometries with the intent of motivating the reader to look beyond commonly accepted norms.

An outline of the process used to develop a correlated material model was described. This included the stress-strain material definition as well as the steps necessary to characterize the surface response of the material damage under various load conditions. The practical implementation of the described phenomenological approach using damage as a failure criterion within Abaqus was illustrated using the simulation of drawing and ironing of a blank into a cup.

7. References

1. Tadmor, Ellad B. and Ronald E. Miller: “Modeling Materials: Continuum, Atomistic and Multiscale Techniques”, Cambridge University Press, New York, NY, 2011.

2. Tang, Sing C., Jwo Pan: “Mechanics Modeling of Sheet Metal Forming”, SAE International, Warrendale, PA, 2007.

3. Abaqus Users Manual, Version 6.13-1, Dassault Systémes Simulia Corp., Providence, RI.